

Detailed validation of two deterministic models of prompt emission. Systematic behaviours of residual quantities from the sequential emission

Anabella Tudora ^{1,*}

¹ University of Bucharest, Faculty of Physics, Ro-077125 Bucharest-Magurele, Romania

Abstract. The results of the PbP and sequential emission modellings describe very well the recent experimental data of $^{235}\text{U}(n,f)$. The application of the sequential emission treatment to 49 fission cases has emphasized systematic behaviours of different quantities characterizing the fragments and the prompt emission. These allowed the determination of a general form of the residual temperature distribution for each emission sequence and the inclusion of sequential emission into the Los Alamos model.

1 Basic features of the Point-by-Point and sequential emission modellings

Detailed descriptions of both models were already reported, see Ref.[1] and references therein for the Point-by-Point (PbP) model and Ref.[2] for the sequential emission treatment. Consequently only a few basic features, showing the similarities and differences between these modellings, are briefly mentioned in the following.

Both models work with the same fragmentation range, which is deterministically constructed as following. The initial fragment mass range is going from symmetric fission up to a very asymmetric split (with a step of 1 mass unit). For each mass number A , three or five charge numbers Z are taken into account, as the nearest integer values above and below the most probable charge $Z_p(A) = Z_{UCD}(A) + \Delta Z(A)$. The isobaric charge distribution is taken as a narrow Gaussian centred on $Z_p(A)$. For each fragmentation the calculations are done at TKE values covering a large range (e.g. from 100 to 200 MeV) with a step size of 5 MeV or even less (e.g. 1 or 2 MeV). Both models use the same TXE partition based on modelling at scission ([1, 3] and references therein), which consists of the calculation of the extra-deformation energy of fragments at scission compared to full acceleration, and the partition of the available excitation energy at scission under the assumptions of statistical equilibrium at scission and level density of nascent fragments in the Fermi-gas regime.

In the PbP model the sequential emission is globally taken into account by a residual temperature distribution $P(T)$ on which the neutron evaporation spectrum in the centre-of-mass frame at a given residual temperature is integrated. In the PbP model the compound nucleus cross-section of the inverse process $\sigma_c(\epsilon)$ is provided by optical model calculations

* Corresponding author: anabellatudora@hotmail.com

with phenomenological parameterisations adequate for nuclei appearing as fragments (e.g. Becchetti-Greenlees, Koning-Delaroche). Other prescriptions for $\sigma_c(\epsilon)$ are possible, too, e.g. analytical expressions of $\sigma_c(\epsilon)$ or even a constant $\sigma_c(\epsilon)$. The PbP model can work with different prescriptions for the level density parameter of fragments, but usually energy-dependent level density parameters provided by the super-fluid model are employed.

The sequential emission treatment is based on the successive equations of residual temperature, which are solved for each emission sequence k corresponding to each initial fragment A, Z at each TKE value [2]. These recursive equations are solved under the approximations of non-energy dependent level density parameters of fragments, e.g. provided by the Egidy-Bucurescu systematic for the back-shift Fermi-gas (BSFG) model, and an analytical expression of $\sigma_c(\epsilon)$ (see Ref.[2], for details).

The primary results of the PbP model are the multi-parametric matrices of different quantities, generically labelled $q(A,Z,TKE)$ (e.g. prompt neutron multiplicity $\nu(A,Z,TKE)$, prompt γ -ray energy $E\gamma(A,Z,TKE)$, average prompt neutron energy in the centre-of-mass frame $\langle \epsilon \rangle(A,Z,TKE)$ etc.). In the sequential emission treatment the matrix $q(A,Z,TKE)$ is obtained by averaging the quantities corresponding to each sequence $q_k(A,Z,TKE)$ over the number of sequences $k_{max}(A,Z,TKE)$ associated to each initial fragment at each TKE value.

2 Detailed validation of these modellings

The first and most relevant validation of a prompt emission model consists of the comparison of the multi-parametric matrices for different quantities (e.g. $\nu(A,TKE)$, $E\gamma(A,TKE)$, etc.) with the experimental data. This comparison *validates the prompt emission model itself* because the fragment distribution $Y(A,TKE)$ is not involved.

The comparison of different single distributions of prompt emission quantities (e.g. $\nu(A)$, $\nu(TKE)$, $\langle \epsilon \rangle(A)$ etc.) and of total average quantities (e.g. $\langle \nu_p \rangle_{tot}$, $\langle E\gamma \rangle$, prompt neutron spectrum in the centre-of-mass and laboratory frames, etc.) with the experimental data *validates the prompt emission model together with the $Y(A,TKE)$ distribution* (on which the primary results, i.e. $q(A,TKE)$, are averaged).

The primary model results, i.e. multi-parametric matrices of different quantities, can be compared in detail with the existing experimental data, using the following 2D representations (a) the quantity as a function of TKE for a given fragment mass and (b) the quantity as a function of A for a given TKE value.

The recent experimental data of $\nu(A,TKE)$ for $^{235}\text{U}(n,f)$ measured by Göök et al. [4] offer the possibility to validate the PbP and sequential emission models themselves.

Fig.1 shows these $\nu(A,TKE)$ data in the 2D representation denoted by (a) (exemplified for nine fragment mass pairs), which are compared in the upper part with the PbP calculation performed in 2017 [1] and in the lower part with the sequential emission calculation also previously reported [2]. A comparison of the $\nu(A,TKE)$ data in the 2D representation denoted by (b) (open squares) with the results of PbP (red circles) and sequential emission (blue stars) is illustrated in **Fig.2** for four values of TKE. The excellent description of the $\nu(A,TKE)$ data of Ref.[4] by the PbP model result is easily seen. In the case of sequential emission treatment, the agreement with the data is also good but not so remarkable as in the case of PbP. This fact, as well as the staggering observed in a part of $\nu(A,TKE)$ results of sequential emission (in both 2D representations) is due to the limited number of initial fragments, which are taken into account in the deterministic construction of the initial fragmentation range. In the case of PbP even if the fragmentation range is the same, this situation is avoided by the global treatment of the sequential emission using the residual temperature distribution $P(T)$ which covers the entire process of successive neutron emission corresponding to each initial fragment.

Consequently the $\nu(A, TKE)$ results for $^{235}\text{U}(\text{n}_{\text{th}}, \text{f})$ provided by the PbP and sequential emission modellings reported in Refs. [1, 2] are confirmed by the subsequent measurements of Gök et al. [4]. This fact can be considered as a valuable validation of both models.

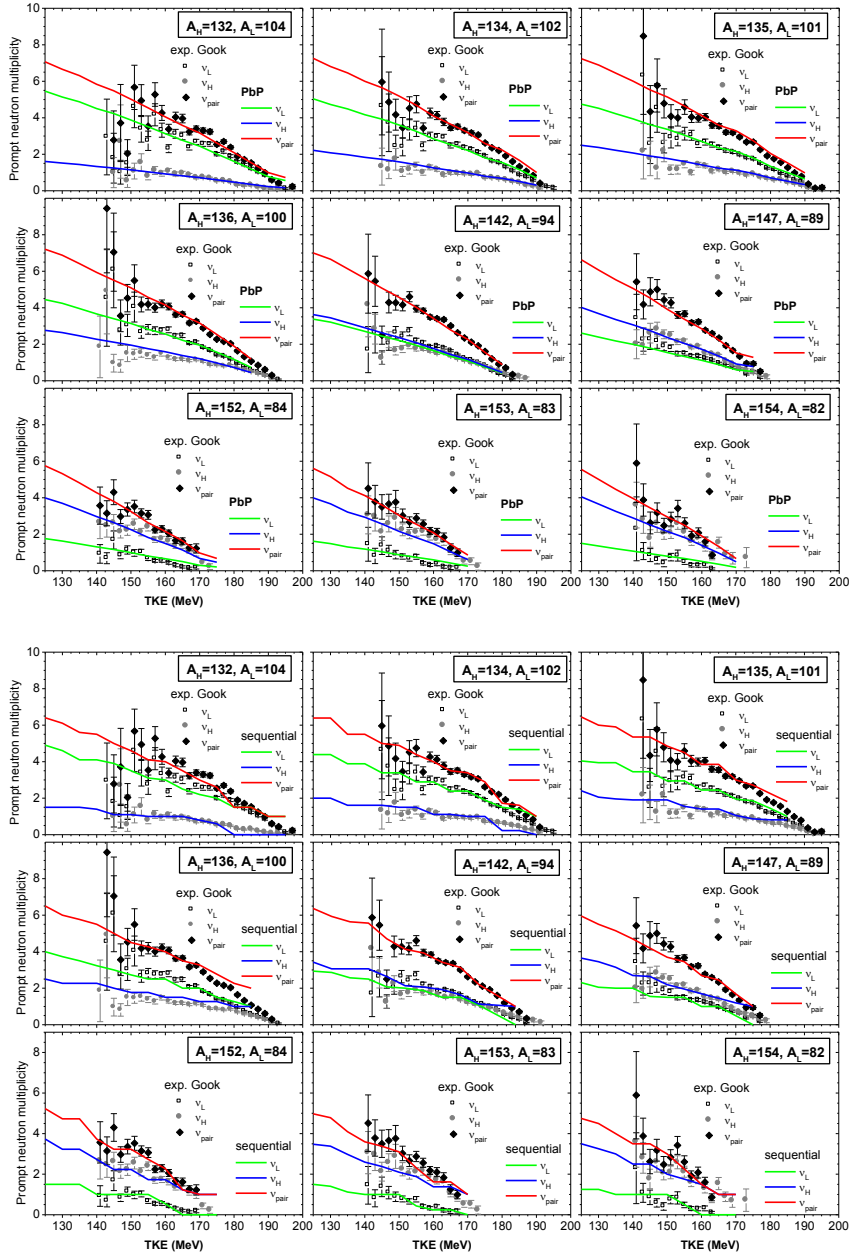


Fig.1. Comparison of the $\nu(A, TKE)$ results of PbP (upper part) and sequential emission (lower part) with the recent data of Gök et al. in the representation as $\nu(TKE)$ for a given fragment mass.

PbP and sequential emission results of single distributions of different quantities, describing well the existing experimental data, were already reported, see Refs. [2, 3] and references therein.

The comparison of model results for the prompt neutron spectrum in the centre-of-mass frame $\Phi(\varepsilon)$ with experimental data deserves a special mention because the data for this quantity are almost inexistent. Fortunately the recent experimental $\Phi(\varepsilon)$ data reported in Ref.[4] offer this possibility.

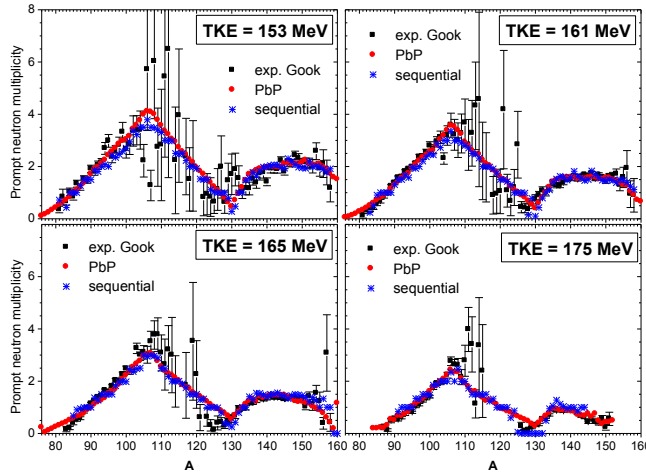


Fig.2. Comparison of the $\nu(A, TKE)$ results of PbP (red circles) and sequential emission (blue stars) with the recent data of Gök et al. (black squares) in the representation as $\nu(A)$ at a given TKE value (which is indicated in each frame).

As an example, **Fig.3** shows the very good description of experimental $\Phi(\varepsilon)$ data for selected fragment mass ranges around the most probable fragmentation [4] (light fragments in the upper part and heavy fragments in the lower part) by the PbP results [1] (representing the spectrum obtained by averaging over the light and heavy fragment groups, respectively).

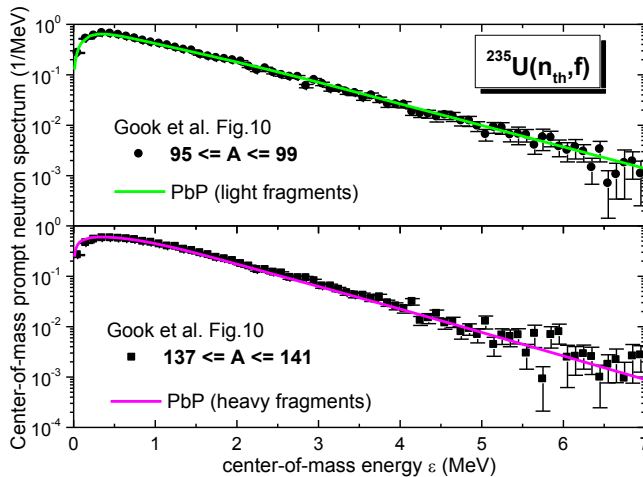


Fig.3. Experimental prompt neutron spectrum in the centre-of-mass frame for selected fragment mass ranges around the most probable fragmentation of Gök et al. in comparison with the PbP result.

3 Systematic behaviours of residual quantities resulting from the sequential emission treatment and possible applications (preliminary results)

As it was mentioned in Ref.[2] the development of a sequential emission modelling has had as initial goal the determination of a general form for $P(T)$ needed in prompt emission models with a global treatment of the sequential emission, like PbP and Los Alamos (LA). For this reason the sequential emission modelling was applied to many fissioning systems benefiting of reliable experimental $Y(A, TKE)$ data, i.e. the spontaneous fission of ^{252}Cf and of even-even isotopes $^{236-244}\text{Pu}$, the thermal neutron induced fission of ^{235}U , ^{233}U and ^{239}Pu and the fast neutron induced fission of ^{234}U , ^{238}U and ^{237}Np , at incident energies below the threshold of the second chance fission. This means a total number of 49 fission cases covering a large range of fissioning nuclei and TXE values. A first finding, reported in Ref.[2], refers to the total average residual temperatures $\langle T \rangle$ (corresponding to the sum of residual temperature distributions following the successive emission of all neutrons from the light and heavy fragments and from all fragments) which can be related only to the average temperature of initial fragments $\langle T_i \rangle$. I.e. the ratios $\langle T \rangle / \langle T_i \rangle$ are the same, of about 0.6, for all studied cases irrespective of the prescriptions used for $\sigma_c(\epsilon)$ and the level density parameters of initial and residual fragments.

The study of such systematic behaviours is in progress. It was ascertained that for each emission sequence (indexed k) the ratios $\langle T_k \rangle / \langle T_i \rangle$ are almost the same for all studied fission cases irrespective of the prescriptions used for $\sigma_c(\epsilon)$ and the level density parameters. This fact is illustrated in the left part of **Fig.4** where the ratios $\langle T_k \rangle / \langle T_i \rangle$ of the studied cases are plotted as a function of TXE with different symbols (corresponding to the emission sequences k from 1 to 6). The constant values approximating these calculated ratios for each emission sequence are represented by horizontal lines plotted with the same colours as the respective symbol.

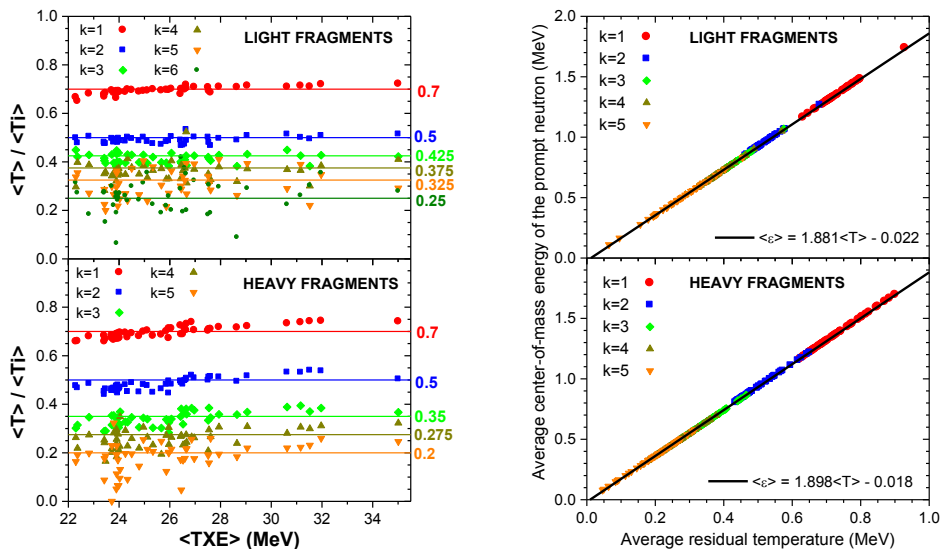


Fig.4. Left part: the ratios $\langle T_k \rangle / \langle T_i \rangle$ as a function of TXE resulting from the sequential emission calculations (different symbols corresponding to each sequence) and the constant values approximating these ratios (lines plotted with the same colour as the respective symbol). Right part the average centre-of-mass energy of each emitted neutron $\langle \epsilon \rangle_k$ as a function of $\langle T_k \rangle$ (using the same symbols and colours as in the left part) and its linear fit (black line).

The ratios of the average residual energy to the initial excitation energy $\langle E_r^{(k)} \rangle / \langle E^* \rangle$ corresponding to each emission sequence are also almost the same for all investigated fission cases, irrespective of the prescriptions used for the level density parameters and $\sigma_c(\varepsilon)$. Similar to the total average temperature ratio $\langle T \rangle / \langle T_i \rangle$ which is of about 0.6 in all cases [2], the ratios of the total average residual energy $\langle E_r \rangle$ to $\langle E^* \rangle$ is also the same, of about 0.43, for all studied fissioning systems.

Linear correlations between the average centre-of-mass energy of each emitted prompt neutron $\langle \varepsilon \rangle_k$ and the corresponding average residual temperature $\langle T_k \rangle$ and between $\langle \varepsilon \rangle_k$ and the root-square of $\langle E_r^{(k)} \rangle$ are also observed. The slopes of these linear dependences allow the determination of global values for the total average level density parameter of the light and heavy fragment groups, which are in good agreement with the general trend of the average level density parameters of the studied cases. Correlations of the average energy carried away per neutron ($\langle \eta_k \rangle = \langle \varepsilon \rangle_k + \langle S_n \rangle_{k-1}$) with different quantities characterizing the fragments (e.g. the average neutron separation energy, the average residual temperature etc.) are also obtained.

The constant values of the ratios $\langle T_k \rangle / \langle T_i \rangle$ and $\langle E_r^{(k)} \rangle / \langle E^* \rangle$ together with the linear dependence of $\langle \varepsilon \rangle_k$ on $\langle T_k \rangle$ can provide indicative values of $\langle T \rangle$, $\langle E_r \rangle$, $\langle \varepsilon \rangle$, $\langle \eta \rangle$ without to use prompt emission models. E.g. if the average initial temperatures of the light and heavy fragment groups $\langle T_i \rangle_{L,H}$ or of all fragments $\langle T_i \rangle$ are known for a given fissioning system then $\langle \varepsilon \rangle_{L,H}$ or $\langle \varepsilon \rangle$ can be obtained from the linear dependence of $\langle \varepsilon \rangle$ on $\langle T \rangle$ (right part of Fig.4) by using the ratio $\langle T \rangle / \langle T_i \rangle \approx 0.6$ [2]. As an example for $^{252}\text{Cf}(\text{SF})$: $\langle \text{TXE} \rangle = 35$ MeV and the equivalent initial temperature $\langle T_i \rangle = (\langle \text{TXE} \rangle / \langle a \rangle)^{1/2}$ based on the average level density parameter which is simply taken as $\langle a \rangle = 252/11 \text{ MeV}^{-1}$ lead to $\langle \varepsilon \rangle = 1.382$ MeV which is in a reasonable agreement with the experimental data.

1.2 Inclusion of the sequential emission into the Los Alamos model

The constant values of the temperature ratios referring to each emission sequence (plotted in the left part of Fig.4), i.e. $r_k = \langle T_k \rangle / \langle T_i \rangle$, allow to define a residual temperature distribution $P_k(T)$ for each emission sequence, having a triangular form with a sharp cut-off at high temperatures [2] and the maximum temperature given by $T_{\text{max}}^{(k)} = (3/2)r_k \langle T_i \rangle$. This fact makes possible the inclusion of sequential emission into the LA model. In this case the spectrum in the centre-of-mass frame corresponding to each prompt neutron emitted successively from the light or heavy fragment of the most probable fragmentation is calculated as

$$\Phi_k(\varepsilon) = \int_0^{T_{\text{max}}^{(k)}} \varphi(\varepsilon, T) P_k(T) dT \quad (1)$$

In order to determine the input parameters of the LA model, as average values corresponding to the most probable fragmentation, different prescriptions can be used, concerning: *i*) $\sigma_c(\varepsilon)$ (provided by optical model calculation, analytical expression or constant), *ii*) different methods of TXE partition, *iii*) the level density parameters of fragments (e.g. energy-dependent provided by the super-fluid model or non-energy dependent provided by different systematics, etc.).

An example of prompt neutron spectra in the centre-of-mass frame provided by the LA model including the sequential emission is given for $^{235}\text{U}(\text{n}_{\text{th}}, \text{f})$ in **Fig.5** where the centre-of-mass spectrum of the first emitted neutron is plotted with a blue dashed line and of the second emitted neutron with a green dash-dotted line. The total centre-of-mass spectrum (obtained by averaging the spectra of each emitted neutron over the probability for emission of each neutron Pn_k [2]) is plotted with a red solid line. As it can be seen it describes very

well the experimental data of Gök et al. [4]. Note, in this example the following prescriptions were used: $\sigma_c(\epsilon)$ from optical model calculations with the Becchetti-Greenlees parameterisation, the TXE partition from modelling at scission ([1, 3] and references therein) and level density parameters provided by the super-fluid model.

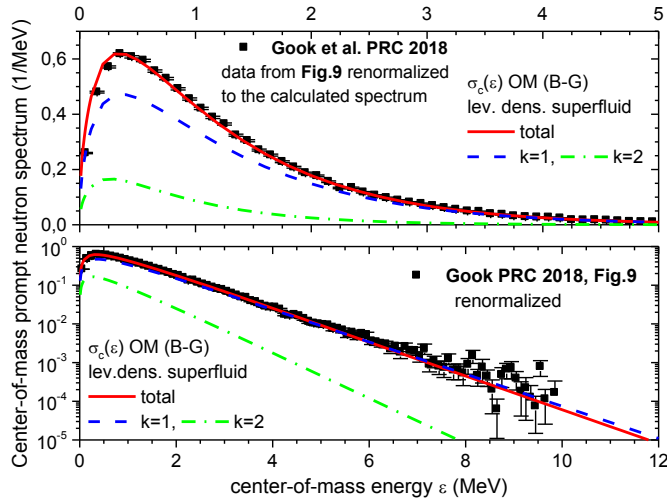


Fig.5: LA model calculation of the centre-of-mass spectrum for the first emitted neutron (dashed blue line), the second emitted neutron (green dash-dotted line) and the total centre-of-mass spectrum (solid red line) in comparison with the experimental data of Gök et al. [4] (black squares).

4 Conclusions

The very good description of the recent prompt emission data of Gök et al. [4] (especially those of prompt neutron multiplicity as a function of A and TKE) by the results of the PbP and sequential emission modellings previously reported [1, 2], constitutes a valuable validation of these models.

The application of the deterministic treatment of sequential emission [2] to 49 fission cases (covering a large range of fissioning nuclei and excitation energies) emphasized systematic behaviours of different average quantities characterizing the initial and residual fragments and the prompt emission. The systematics concerning the average residual temperatures allowed to define a general form of the residual temperature distribution associated to each emission sequence $P_k(T)$. This fact makes possible the inclusion of sequential emission into the Los Alamos model of prompt emission.

Acknowledgements: this work was done in the frame of the Romanian research project PN-III-P4-PCE-2016-0014 (contract 7/2017).

References

1. A. Tudora, F.-J. Hamsch, Eur. Phys. J. A **53**, 159 (2017)
2. A. Tudora, F.-J. Hamsch, V. Tobosaru, Eur. Phys. J. A **54**, 87 (2018)
3. R. Capote et al., Nucl. Data Sheets **131**, 1-106 (2016)
4. A. Gök, F.-J. Hamsch, S. Oberstedt, M. Vidali, Phys. Rev. C (2018) (to be published)